

SPECTROSCOPIC PROPERTIES AND COLLECTIVITY BEYOND $^{132}\text{Sn}^*$

HOUDA NAÏDJA^{a,b,c}, FRÉDÉRIC NOWACKI^a

^aUniversité de Strasbourg, CNRS, IPHC UMR 7178, 67000 Strasbourg, France

^bGSI Helmholtzzentrum für Schwerionenforschung GmbH
64291 Darmstadt, Germany

^cUniversité Constantine 1, LPMS, route Ain El Bey 25000 Constantine, Algeria

(Received December 14, 2016)

Recent shell-model advances in the mass region above the doubly closed core ^{132}Sn are reported in the present work. Using an effective interaction based on the N3LO potential, the low-lying spectra, E2 and M1 transition strengths are calculated for the following nuclei: $^{134,136,138}\text{Te}$, $^{136,138,140}\text{Xe}$, $^{138,140,142}\text{Ba}$, $^{140,142,144}\text{Ce}$ and $^{142,144,146}\text{Nd}$. We focus in the discussion on the collectivity in the $N = 86$ isotones characterized by development of triaxial γ bands.

DOI:10.5506/APhysPolB.48.587

1. Introduction

The mass region above ^{132}Sn core represents an interesting area for experimental [1–8] and theoretical [9–13] nuclear structure research. In our earlier shell-model works [1, 12, 13], we have calculated the energy levels, the isomeric transitions and the masses of $^{134,136,138,140}\text{Sn}$. In the present work, we have progressed in our investigation of this region by describing the spectroscopic properties of even–even chains of nuclei with $52 \leq Z \leq 60$ and $82 \leq N \leq 86$ using an effective interaction based on the N3LO potential (named N3LOP) reported in Section 3.1. The presence of the collectivity in the $N = 86$ isotones is widely discussed in Section 3.2, where the quadrupole properties sign the presence of triaxial γ bands.

2. Shell-model overview

Thereafter we carry shell-model calculations in the natural valence space spanned by $1f_{7/2}, 0h_{9/2}, 1f_{5/2}, 2p_{3/2}, 2p_{1/2}, 0i_{13/2}$ orbitals for neutrons and

* Presented at the Zakopane Conference on Nuclear Physics “Extremes of the Nuclear Landscape”, Zakopane, Poland, August 28–September 4, 2016.

$0g_{7/2}, 1d_{5/2}, 1d_{3/2}, 2s_{1/2}, 0h_{11/2}$ orbitals for protons, above an inert closed ^{132}Sn core (hereafter denoted by $r4h-r5i$ [14]). The numerical treatment of such a valence space is very challenging. We face, for example, matrix diagonalizations with basis dimensions up to $\sim 2 \cdot 10^{11}$ Slater determinants for the case of ^{146}Nd . The calculations are carried out using Antoine and Nathan shell-model codes [15, 16].

As a starting point, we have employed a realistic interaction derived from chiral effective field theory potentials [17] noted by N3LO. Its repulsive short range has been renormalized with the use of the so-called low momentum potential $V_{\text{low } k}$ procedure, defined within a cutoff $\Lambda = 2.2 \text{ fm}^{-1}$. It is then adapted to the model space by many-body perturbation theory techniques, including all the \hat{Q} -box folded diagrams up to the second order [18]. The corresponding neutrons and protons single-particle energies are fixed from ^{133}Sn and ^{133}Sb experimental values [19].

The initial N3LOP realistic interaction fails in reproducing the isomeric transition strength in ^{136}Sn , and we have reduced the diagonal and off-diagonal $f_{7/2}$ pairing matrix elements of the neutron–neutron part. This was already identified as a seniority mixing effect [1, 12, 13]. We denote this final interaction hereafter by N3LOP, and we apply it to survey the properties of open neutron–proton systems close to ^{132}Sn .

3. Applications and results

3.1. Energy levels, E2 and M1 transitions

The calculated low-energy levels of different nuclei displayed in Figs. 1–5 (solid lines), show a remarkable good agreement compared to the observed values taken from [19] (dotted lines). A compression in the levels schemes is visible with increasing neutron number, indicating the presence of collectivity in this mass region (see Section 3.2). In the following, the electromagnetic transitions are calculated with the use of $0.6e$ for neutrons and $1.6e$ for protons effective charges for E2 operators, spin and orbital g factors for protons $(g_{\pi}^s, g_{\pi}^l) = (4.189, 1.1)$ and neutrons $(g_{\nu}^s, g_{\nu}^l) = (-2.869, -0.1)$ for M1 operators. The electric transitions $B(\text{E}2, 2^+ \rightarrow 0^+)$ for several nuclei are reported in Fig. 6. An impressive agreement is found with the experimental data from [19] within error bars. The only exception is the case of ^{136}Te where the calculated value is overestimated compared to the measured one. The anomaly in this nucleus was already observed and discussed extensively in Refs. [9, 11, 20]. In addition, there is a clear increase in the transitions strength with increasing neutron number, reflecting the transition from spherical character in the $N = 82$ isotones to a collective one in the $N = 86$ isotones. For the magnetic moments of 2^+ states, an overall good agreement is seen in Fig. 7.

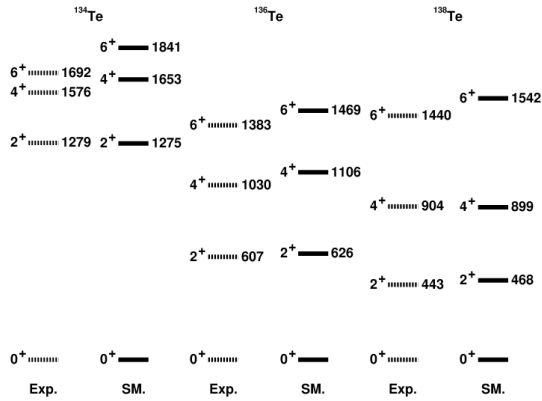


Fig. 1. The low-lying energy levels of Te isotopes.

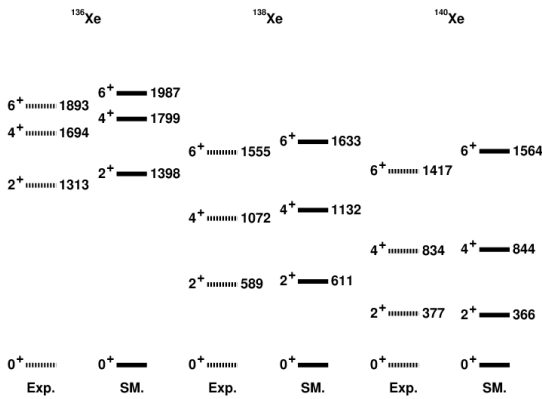


Fig. 2. The low-lying energy levels of Xe isotopes.

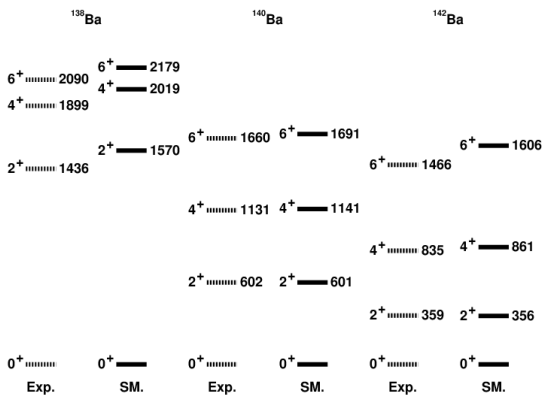


Fig. 3. The low-lying energy levels of Ba isotopes.

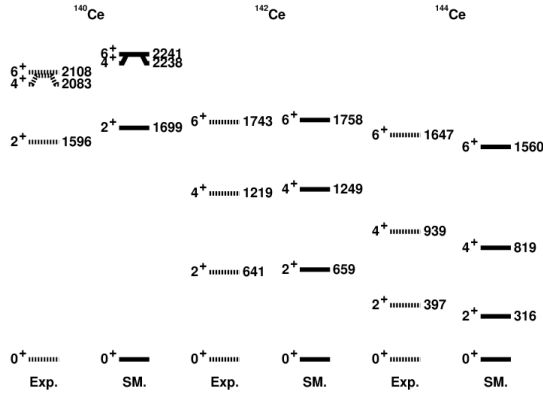


Fig. 4. The low-lying energy levels of Ce isotopes.

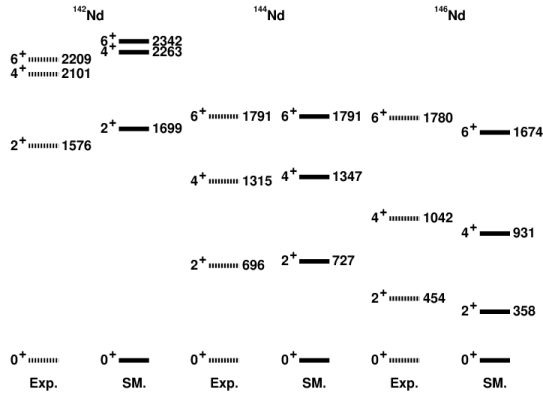


Fig. 5. The low-lying energy levels of Nd isotopes.

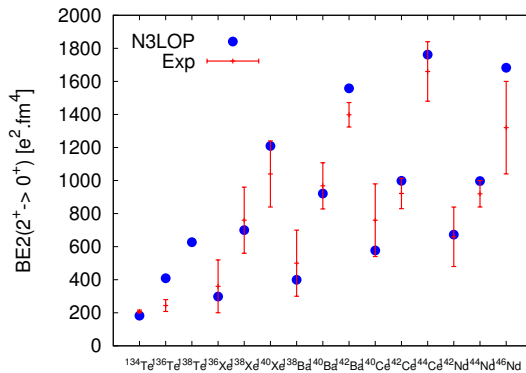


Fig. 6. Variation of $E2$ transitions from 2^+ to 0^+ for different nuclei.

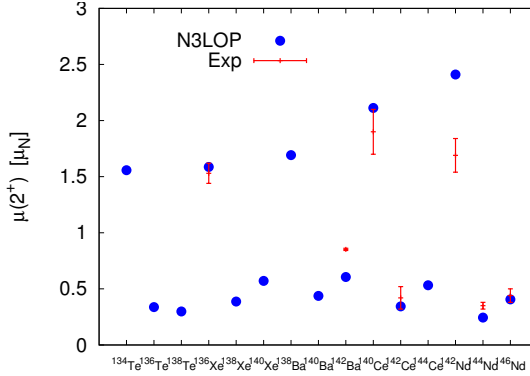


Fig. 7. Variation of magnetic moment of 2^+ state for different nuclei.

3.2. Collectivity in the $N = 86$ isotones

In this section, we focus on the $N = 86$ isotonic chain *i.e.* ^{138}Te , ^{140}Xe , ^{142}Ba , ^{144}Ce , ^{146}Nd . It is characterized by very strong $B(E2, 2^+ \rightarrow 0^+)$ strength transitions (see Fig. 6), which indicate the presence of large quadrupole correlations. Moreover, the inspection of calculated spectroscopic quadrupole properties in these systems reveals striking features. Indeed,

- $Q_s(2^+_\gamma, K = 2)$ is more or less equal and of opposite sign to $Q_s(2^+_\gamma, K = 0)$,
- $Q_s(3^+, K = 2) \simeq 0$, and the low-lying 3^+ state is connected by a strong transition to the 2^+_γ state.

All these points seen in the $N = 86$ isotonic chain (see Figs. 8 and 9), sign the presence of triaxial γ bands. The band is in all the cases built on the 2^+_γ band-head state. There is also an apparent gradual increase of deformation from ^{138}Te to ^{146}Nd , reaching a maximum in ^{144}Ce .

In order to provide a complete vision about the deformation and the degree of the collectivity in these systems, we use the Kumar geometric model [21], to extract the β axial deformation parameter and γ triaxial angle, and get more relevant information about intrinsic shapes. From the set of β and γ values ascribed to the $N = 86$ isotones, we observe in Fig. 10

- mild deformation in ^{138}Te ,
- clear increase of deformation and non-axiality from ^{140}Xe to ^{146}Nd with a maximum in ^{144}Ce .

This enhancement of the collectivity is interpreted as a result of the pseudo-SU(3) symmetry structure of the $g_{7/2}$, $d_{5/2}$, $d_{3/2}$, $s_{1/2}$ proton orbits [22], and the quasi-SU(3) symmetry structure of the $f_{7/2}$, $p_{3/2}$ neutron orbits sequence [23, 24].

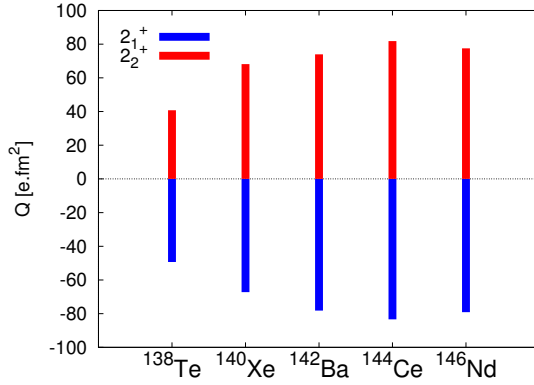


Fig. 8. The quadrupole moments of 2_1^+ and 2_2^+ states for the $N = 86$ isotones.

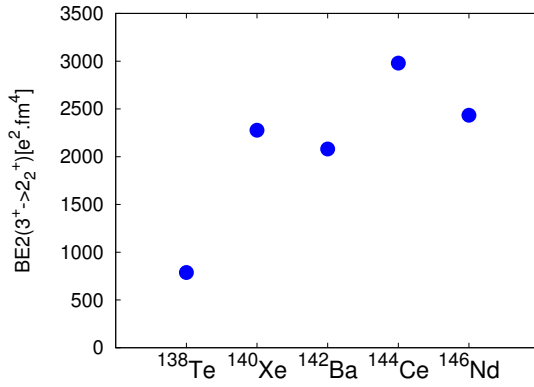


Fig. 9. Variation of E2 transition rates from 3^+ to 2_2^+ for the $N = 86$ isotones.

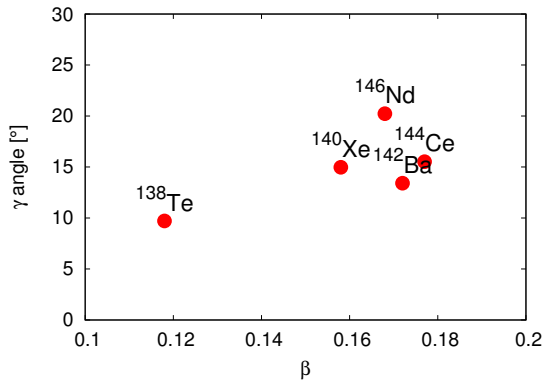


Fig. 10. β deformation parameter and γ angle for the $N = 86$ isotones.

4. Conclusions

Within the shell-model framework, we have investigated the spectroscopic properties and the transition rates of even–even neutron-rich nuclei beyond ^{132}Sn . Our calculations reproduce quite accurately the behavior of the measured energy levels and the electromagnetic transitions. In addition, the signs of collectivity in the nuclei: ^{138}Te , ^{140}Xe , ^{142}Ba , ^{144}Ce and ^{146}Nd were discussed and shown with the signature of triaxial γ bands. The evolution of this collectivity is sensitive to SU(3) symmetries (or their approximations) of the neutrons and protons orbits sequences, reaching a maximum in ^{144}Ce . The deformation in this chain of nuclei can be considered as a transition regime, from low deformation to stronger one, already observed experimentally in rare-earth nuclei. This study is a stringent test of N3LOP effective interaction recently developed for this mass region and our predictions of the electromagnetic properties and collectivity constitute a benchmark for future experimental investigations.

H.N. acknowledges financial support from the Helmholtz Association through the Nuclear Astrophysics Virtual Institute (VH-VI-417), and IPHC for the numerical calculations support. This work was supported by the Polish National Science Centre (NCN) under contract No. 2013/08/M/ST2/00257 (LEA-COPIGAL).

REFERENCES

- [1] G.S. Simpson *et al.*, *Phys. Rev. Lett.* **113**, 132502 (2014).
- [2] R. Lozeva *et al.*, *Phys. Rev. C* **92**, 024304 (2015).
- [3] P. Lee *et al.*, *Phys. Rev. C* **92**, 044320 (2015).
- [4] Y. Huang *et al.*, *Phys. Rev. C* **93**, 064321 (2016).
- [5] A.J. Mitchell *et al.*, *Phys. Rev. C* **93**, 014306 (2016).
- [6] B. Bucher *et al.*, *Phys. Rev. Lett.* **116**, 112503 (2016).
- [7] R. Lozeva *et al.*, *Phys. Rev. C* **93**, 014316 (2016).
- [8] W. Urban *et al.*, *Phys. Rev. C* **93**, 034326 (2016).
- [9] D. Bianco *et al.*, *Phys. Rev. C* **88**, 024303 (2013).
- [10] S. Sarkar, M. Saha Sarkar, *Phys. Rev. C* **81**, 064328 (2010).
- [11] A. Covello *et al.*, *Prog. Part. Nucl. Phys.* **59**, 401 (2007).
- [12] H. Naïdja, F. Nowacki, K. Sieja, *J. Phys.: Conf. Ser.* **580**, 012030 (2015).
- [13] H. Naïdja, F. Nowacki, K. Sieja, *Acta Phys. Pol. B* **46**, 669 (2015).
- [14] J. Duflo, A.P. Zuker, *Phys. Rev. C* **59**, R2347 (1999).
- [15] E. Caurier, F. Nowacki, *Acta Phys. Pol. B* **30**, 705 (1999).

- [16] E. Caurier *et al.*, *Rev. Mod. Phys.* **77**, 427 (2005).
- [17] D. Entem, R. Machleidt, *Phys. Rev. C* **68**, 041001 (2003).
- [18] M. Hjorth-Jensen, T.T.S. Kuo, E. Osnes, *Phys. Rep.* **261**, 125 (1995).
- [19] www.nndc.bnl.gov
- [20] N. Shimizu *et al.*, *Phys. Rev. C* **70**, 054313 (2004).
- [21] K. Kumar, *Phys. Rev. Lett.* **28**, 249 (1972).
- [22] E. Caurier, F. Nowacki, A. Poves, K. Sieja, *Phys. Rev. C* **82**, 064304 (2010).
- [23] A.P. Zuker, J. Retamosa, A. Poves, E. Caurier, *Phys. Rev. C* **52**, R1741 (1995).
- [24] A.P. Zuker, A. Poves, F. Nowacki, S.M. Lenzi, *Phys. Rev. C* **92**, 024320 (2015).